

# Simulation of Seismic-Wave Propagation During the 1927 $M_L$ 6.25 Jericho Earthquake

Shahar Shani-Kadmiel<sup>1,3,\*</sup>, Michael Tsesarsky<sup>1,2</sup>, and Zohar Gvirtzman<sup>3</sup>

<sup>1</sup> Department of Geological and Environmental Sciences, BGU; <sup>2</sup> Department of Structural Engineering, BGU; <sup>3</sup> Geological Survey of Israel

## 1. Introduction

The Dead Sea Transform (DST) is the major seismic source in Israel and neighboring countries, with a proven seismic record: geological, archeological and historical. It is estimated to produce up to magnitude 7.5 earthquakes. However, due to the low seismicity rate and the limited deployment of seismological instrumentation, strong earthquakes and their ground motions were not recorded in the region.

The  $M_L$  6.25 July 11, 1927 Jericho earthquake was the most destructive earthquake in the 20th century in the vicinity of Israel and the first significant one to be recorded worldwide. Estimations of casualties range between 250-500 death and 400-700 injuries. Many buildings were damaged (Figure 1), landslides and rockfalls were observed and the flow of the Jordan River had stopped for 21.5 h.

132 Intensity records, based on physical evidences and reports, were compiled by Avni et al., (2002) and re-evaluated by Zohar and Marco (2011) to account for local site-attributes: construction quality, topographic slope, groundwater level, and surface geology (Figure 1).

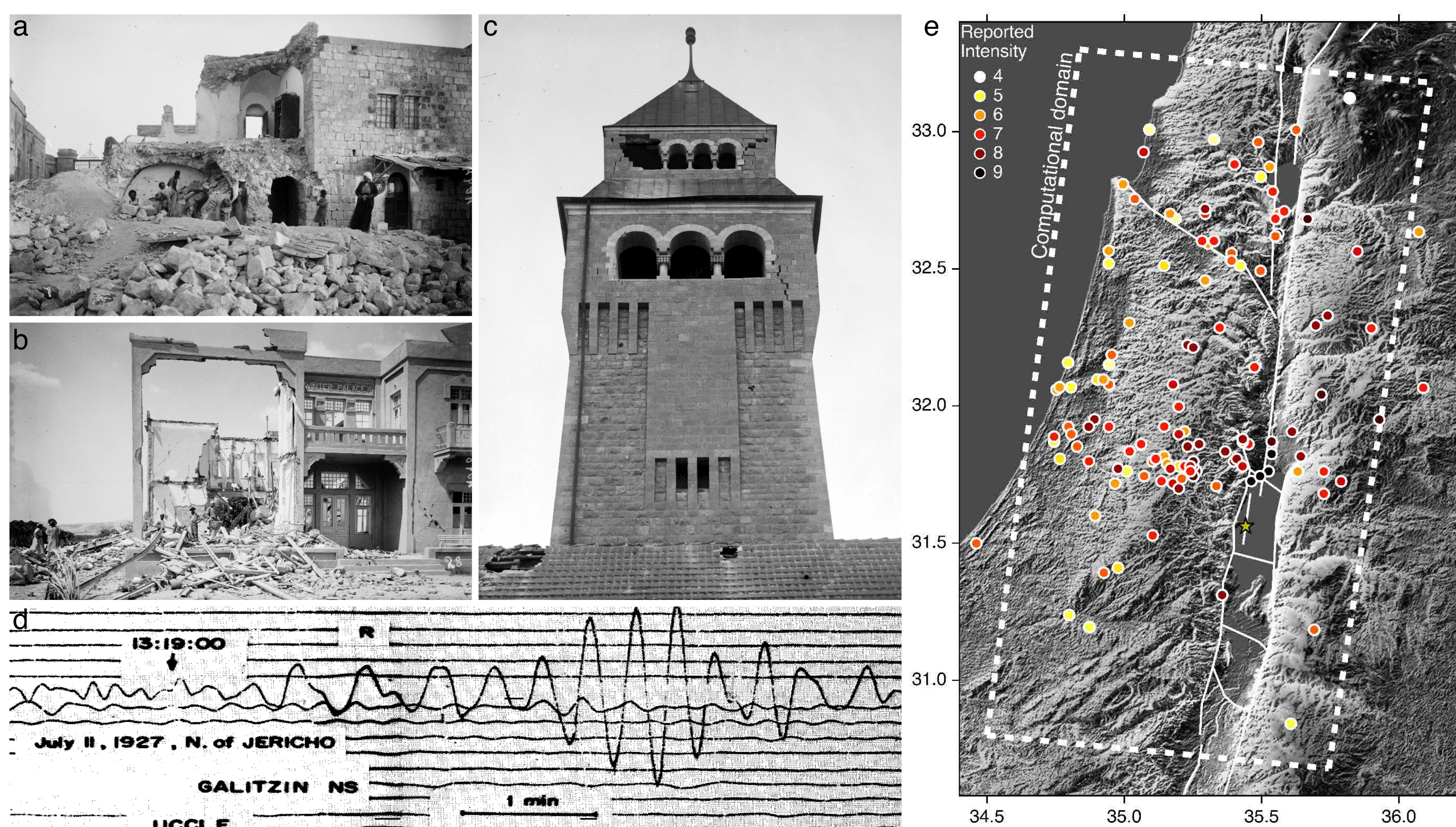


Figure 1: (a), (b) and (c) Structural damage caused by the 1927 Jericho earthquake in Mount of Olives, Jerusalem, Winter Palace Hotel in Jericho, and Augusta Victoria Hospital, respectively. (d) Recorded seismogram of the event at the Royal Observatory of Belgium in Uccle. (e) Reported Intensities (after Zohar and Marco, 2012).

## 2. Research Goals and Methodology

The main goal of our research is to develop a generic and robust finite source model for initiating seismic-wave propagation in simulations of strong earthquakes in regions with low seismicity rate and/or limited instrumental coverage.

To this end we have developed the kinematic Distributed Slip Model (DSM), where slip is distributed over an elliptical rupture patch using a “pseudo-Gaussian” slip-size function (Figure 2). The DSM was implemented in a finite difference code (WPP 2.2) as a pure sinistral strike-slip mechanism rupturing mainly northward. The computational domain was discretized into  $6.3E8$  grid points and 30,000 time steps at a temporal resolution of 6.6 milliseconds were computed. As a first iteration, we used a laterally homogeneous velocity model starting at the surface topography and extending downward for the computational domain (Figure 2).

MMI (Wald et al., 1999) and EMS98/MSK64 (Grünthal, 1998; Medvedev et al., 1964) intensities were calculated based on synthetic seismograms (Figure 3) produced at reported intensity localities and compared to the reported intensities (Figure 4).

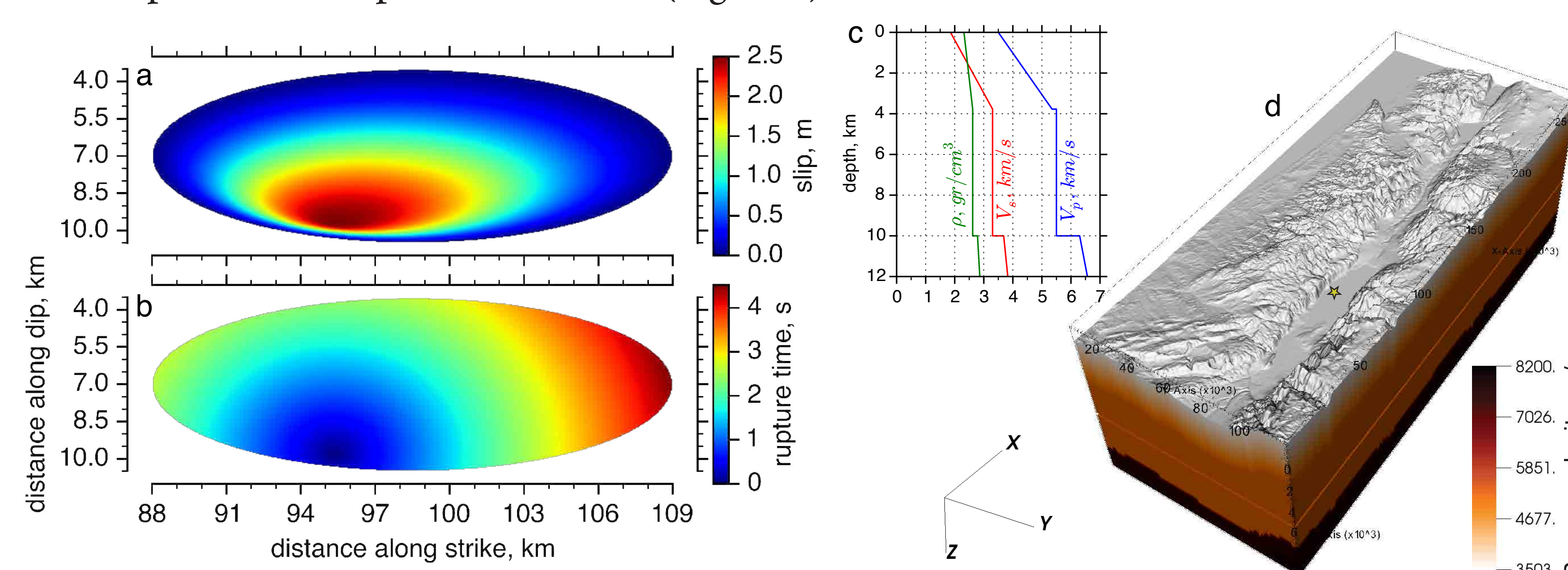


Figure 2: (a) and (b) Slip size and rupture time of the DSM used for initiating seismic-wave propagation. (c) Density and seismic velocities used for the laterally homogeneous seismic model, and (d) the 3D volume with surface topography and P-wave velocity.

## 3. Results

Synthetic seismograms sorted by epicentral distance are presented in Figure 3a and calculated PGV values in Figure 3b. Considering the simplicity of the velocity model, the agreement between the computed and reported seismic intensities is surprisingly good with a mode 0 difference distribution relative to the EMS98 scale and more than 90% of the values within a single intensity unit difference (Figure 4). Intensities computed according to the MMI scale underestimate the reported intensities with mode 1.

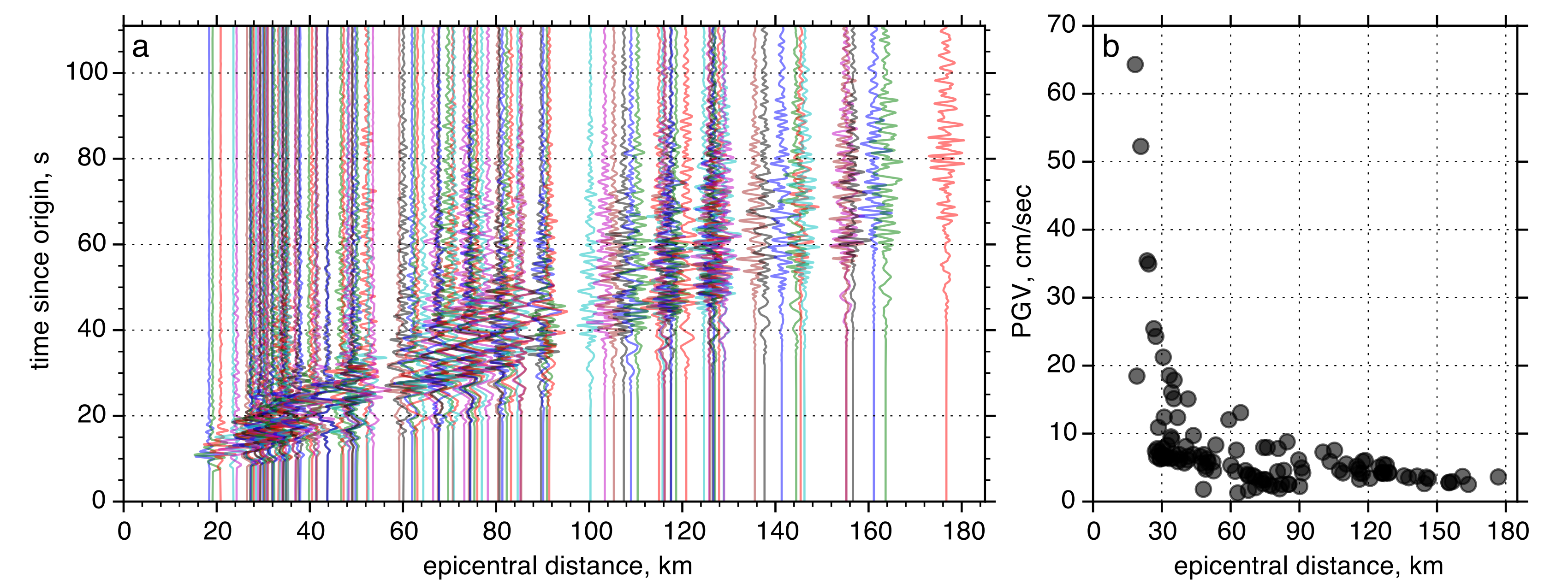


Figure 3: (a) Synthetic seismograms of vertical component ground velocity and (b) calculated PGV at reported localities sorted by epicentral distance.

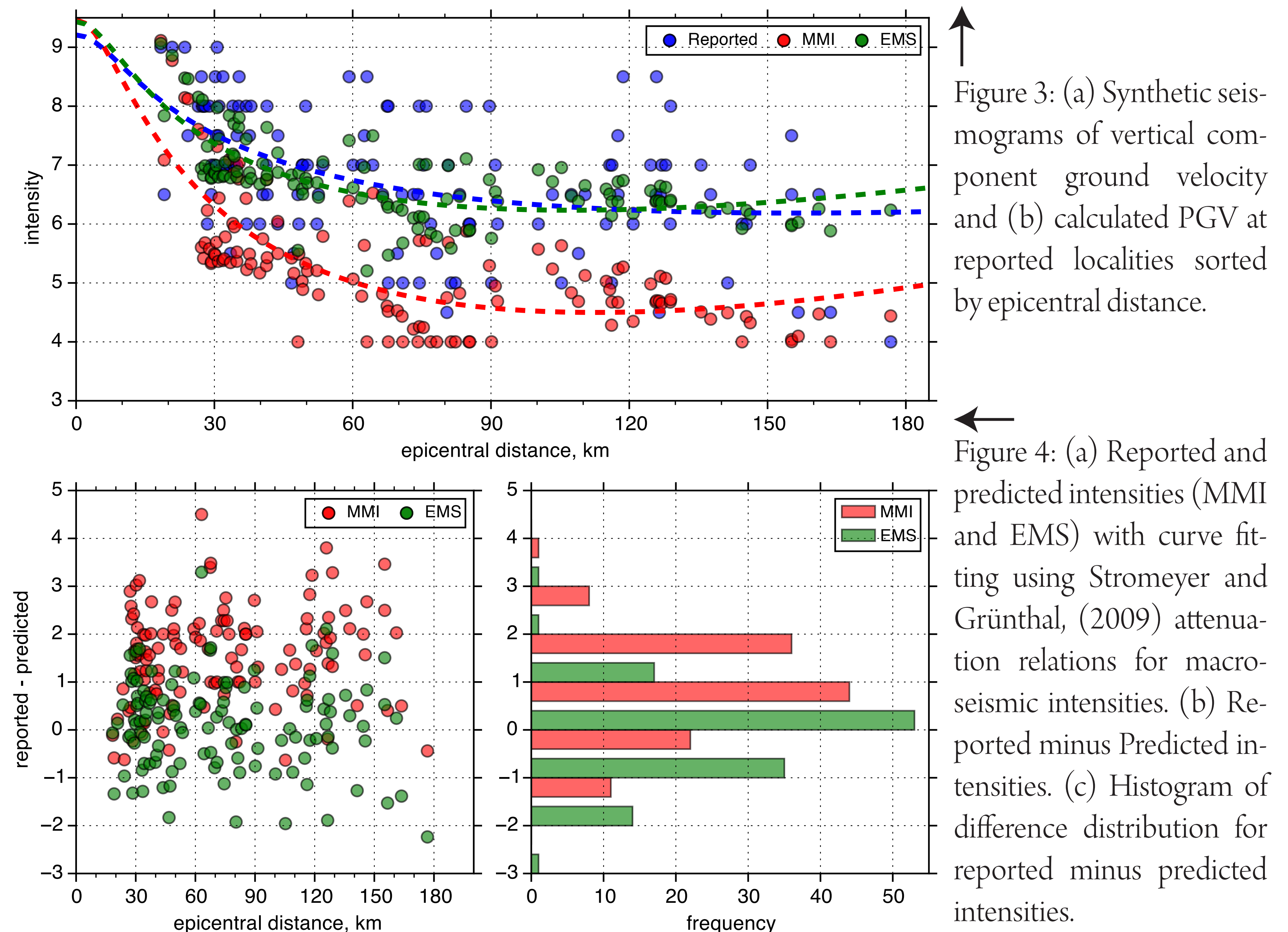


Figure 4: (a) Reported and predicted intensities (MMI and EMS) with curve fitting using Stromeyer and Grünthal, (2009) attenuation relations for macroseismic intensities. (b) Reported minus Predicted intensities. (c) Histogram of difference distribution for reported minus predicted intensities.

## 4. Summary and Conclusions

At a first glance, the seismic radiation pattern and directivity effect of the rupture as depicted by the PGV in Figure 5 explain the reported intensities quite well. This would not have been the case had the fault ruptured southward as previously suggested by Ben-Menahem et al. (1976) and others.

The predicted EMS98/MSK64 values were found to be in agreement with the reported intensity values whereas the predicted MMI values were found to consistently under-predict the reported intensity values.

The discrepancies between the predicted and reported intensity values are attributed to local geological structures and near surface velocity anomalies. We intend to further improve the accuracy of intensity prediction by using increasingly accurate geological models.

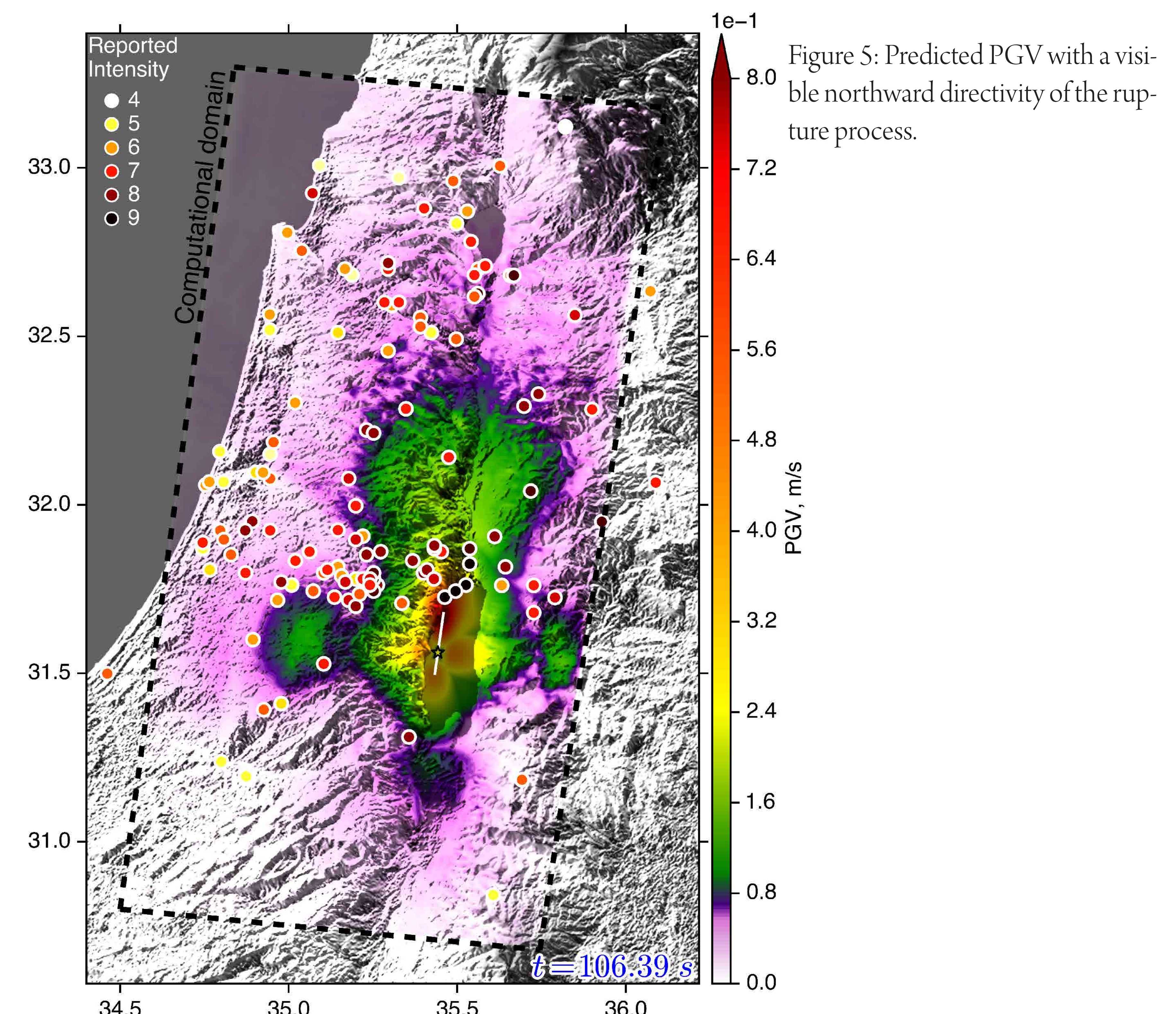


Figure 5: Predicted PGV with a visible northward directivity of the rupture process.

\* Contact: kadmiel@bgu.ac.il (Shahar Shani-Kadmiel)